# ANALYSIS OF DIFFERENT DECAY MODES OF $^{210}Rn^{*}$ NUCLEUS AT ABOVE BARRIER ENERGIES

A Thesis submitted in partial fulfillment of the requirements for the award of degree of

**Masters of Science**

**In**

**Physics**

Submitted by

**KANISHKA SHARMA**

Roll No. 301104008

Under the supervision of

**Dr. MANOJ K. SHARMA**

**Associate Professor**

**SPMS**

**Thapar University, Patiala.**

**School of Physics and Material Science,**

**Thapar University,**

**(Formerly Thapar Institute of Engineering and Technology)**

**Patiala-147004, INDIA**

**July-2013**

*I lovingly dedicate this thesis to my*

*Parents who have always been*

*supportive towards me.*

# CERTIFICATE

I hereby certify that the work which has been presented in this thesis entitled **"Analysis of different decay modes of $^{210}Rn^{*}$ nucleus at above Barrier Energies"** submitted in partial fulfillment of the requirements for the award of degree **of Master of Science in Physics** at **Thapar University, Patiala**, is an authentic record of my own work carried out under the supervision of **Dr. Manoj K. Sharma, Associate Professor, SPMS** and refers other researcher's work which are duly listed in reference section.

The matter embodied in this thesis has not been submitted for the award of any other degree of this or any other university.

Date: 12th July 2013

Kanishka

(Kanishka Sharma)

This is to certify that the above statement made by the candidate is correct and true to best of my knowledge.

12/7/13

**Dr. Manoj K. Sharma**

Associate Professor,

SPMS

Thapar University,

Patiala.

Counter signed by:

Dr. Kulvir Singh

Associate Professor and Head,

School of Physics and Material Science,

Thapar University,

Patiala- 147004

Dr. S.K. Mohapatra,

Dean of Academic Affairs,

Thapar University,

Patiala- 147004.

# ACKNOWLEDGEMENT

With a deep sense of gratitude, I wish to express my sincere thanks to my supervisor, **Dr. Manoj K. Sharma, Associate Professor, SPMS,** for their immense help in planning and executing the work in time. The confidence and dynamism with which **Dr. Manoj K. Sharma** guided the work requires no elaboration. His company and assurance at the time of crisis would be remembered life-long. His valuable suggestions as final words during the course of work are greatly acknowledged. My sincere thanks to him for the help extended to me when I approached him and the valuable discussion that I had with him during the course of thesis.

I express my heartfelt gratefulness **to Mrs. Manpreet Kaur** for extending timely help in carrying out my important works. The co-operation I received from other faculty members of this department is gratefully acknowledged.

I thank GOD, for always being there for me. I also want to thank my family for their support and trust on me whose blessings I will need throughout my life. I also want to thank to my friends and all those people who help me completing my thesis in time.

Date: 12th July 2013

Kanishka

**Kanishka Sharma**

# List of Figures/Tables

# ABSTRACT

Today, in an era of scientific research and technologies, one needs to update his/her knowledge in reference to latest developments in the concerned area. In context of nuclear physics, it becomes very important to have proper understanding of the nuclear reaction dynamics and the related phenomena associated with nuclear structure aspects. Various experimental as well as theoretical efforts are going on to have a better understanding of the nucleus and its properties. The shape and size of the nucleus is very important part in the reaction dynamics as majority of the nuclear systems are deformed to some order. Therefore, to have better understanding of the reaction dynamics, Dynamical cluster model (DCM) has been applied to study the decay patterns of Heavy Mass Nucleus $^{210}$Rn formed in heavy-ion reaction induced using $^{16}$O projectile. The DCM based cross-sections agree fairly with available data by anticipating some Quasi-Fission component at two highest energies. The following reaction is studied and worked upon over a wide range of energies.

$$^{16}O + {}^{194}Pt \rightarrow {}^{210}Rn \rightarrow A_1 + A_2$$

Where $A_1$ and $A_2$ represent the mass of decaying fragments in collective clusterization approach adopted in context of a well known theory known as Quantum Mechanical Fragmentation Theory (QMFT), which was developed in Frankfurt School about four decades from now.

This dissertation consists of three chapters.

**Chapter 1:**

Chapter-1 gives an overview of the nuclear reaction dynamics, associated features such as nuclear shapes, associated decay mechanisms and importance of the work carried out in this dissertation.

**Chapter 2:**

Chapter-2 consists of the description of Dynamical Decay Cluster Model (DCM). It carries the various potentials used in DCM along with other parameters such as preformation factor, barrier penetrability, etc. The deformation effects of nuclear systems are duly included in the framework of DCM.

**Chapter 3:**

Chapter-3 consists of the details of the DCM based calculations for $^{16}O+^{194}Pt\rightarrow^{210}Rn\rightarrow A_1+A_2$ reaction in reference to the possibility of different decay modes over a wide range of incident energies.

# Chapter 1

# Literature Review

# Chapter 1

## 1.1 Introduction:

Nuclear physics is a branch of physics concerned with the structure and behavior of the nucleusand the particles (nucleons) of which it consists. As the name implies, nuclear physics is the study of the nuclei which lie at the core of every atom in the world. Over 99.9% of the mass of all the ordinary matter in the universe is found in the nuclear part of the system. Protons and neutrons (themselves made of quarks) are the building blocks of the nucleus, so a significant effort is made during last few decades to understand the force that holds protons and neutrons together.

A principal research tool of nuclear physics is a high-energy beam of particles, such as protons, neutrons, α-particles or heavy ions, directed as projectiles against nuclear targets. The α-particle is the particle with 2 protons and 2 neutrons composition and refers to the He-nucleus, whereas heavy ions are the nuclear systems having mass greater than α-particle ($A_2 \geq 4$). By analyzing the directions and energies of the recoiling particles and any resulting nuclear fragments, nuclear physicists can obtain details of the reaction dynamics and information about nuclear structure. Beside this, significant amount of efforts are being made to generate concrete information about the strong force that binds nuclear components together, and the release of energy from the nucleus.

The history of nuclear physics as a discipline distinct from atomic physics starts with the discovery of radioactivity by Henri Becquerel in 1896, while investigating phosphorescence in Uranium salts. The discovery of the electron by J. J. Thomson a year later was an indication that the atom had internal structure. At the turn of the 20th century the accepted model of the atom was J. J. Thomson's plum pudding model in which the atom was a large positively charged ball with smallnegatively charged electrons embedded inside of it. By the turn of the century physicists had also discovered three types of radiation emanating from atoms, which they named alpha, beta, and gamma radiation. Experiments in 1911 byOtto Hahn, and by James Chadwick in 1914 discovered that the beta decay spectrum was continuous rather than discrete. That is, electrons were ejected from the atom with a range of energies, rather than the discrete amounts

of energies that were observed in gamma and alpha decays. This was a problem for nuclear physics at the time, because it indicated that energy was not conserved in these decays.

The nucleus was discovered by the New Zealand-born British physicist Ernest Rutherford in 1911 as a result of experiments in firing alpha particles through very thin gold foil. This experiment resulted in one of the most important discoveries of previous century and paved way to investigate a very important branch of Physics termed as Nuclear Physics. To understand the nature and dynamics of nuclei, nuclear reactions play a significant role.

## 1.2 Fusion:

Nuclear fusion is the joining of two nuclei to form a heavier nuclei. The reaction is followed either by a release or absorption of energy. The opposite occurs with nuclear fission. The power of the energy in a fusion reaction can be anticipated by the huge amount of energy released from the sun and a lot of stars in the universe. Nuclear fusion is also applied in nuclear weapons, specifically, a hydrogen bomb.Also, the combination of deuterium & tritium atoms to form helium atoms give rise to such thermonuclear process. For example:

$$^{2}H + {}^{3}H \rightarrow {}^{4}He + {}^{1}n + \text{energy}.$$

Nuclear fusion in heavy-ion collisions is an importantprocess in many phenomena. The fusion of heavy nuclei just above the barrier is an important tool in the production of super-heavy nuclei [1]. The fusion of identical light nuclei at high energies reveals interestingeffects in isolated high-angular-momentum states of the fused system [2]. Nuclear fusion of light nuclei is utilized in accelerator-based heavy-ion inertial fusion for fusion energyproduction [3, 4]. The probability of such interactions depend on the fissility parameter, excitation energy and angular momentum involved.

## 1.3Compound Nuclear Systems

In 1917, Ernest Rutherford was able to accomplish transmutation of nitrogen into oxygen at the University of Manchester, using alpha particles directed at nitrogen $^{14}N + \alpha \rightarrow {}^{17}O + p$. This was the first observation of an induced nuclear reaction, that is, a reaction in which particles from one decayare used to transform another atomic nucleus. Eventually, in 1932 at Cambridge University, a fully artificial nuclear reaction and nuclear transmutation was achieved by Rutherford's colleagues John Cockcroft and Ernest Walton, who used artificially accelerated protons against lithium-7, to split the nucleus into two alpha particles. The feat was popularly known as "splitting the atom", although it was not the modern Nuclear Fission reaction later discovered in heavy elements, in 1938.

A nuclear reaction is a process in which two nuclei or nuclear particles collide to produce products different from the initial particles. In principle, a reaction can involve two or more than two colliding particles, but the probability of three or more nuclei to meet at the same time at the same place is much less than for two nuclei, therefore such an event is exceptionally rare. However, some efforts have been made to explore such possibilities on experimental as well as theoretical front.

When a projectile is hit against a target nucleus, either a low energy projectile is absorbed or a higher energy particle transfers energy to the nucleus, leaving it with too much energy to be fully bound together. On a time scale of about $10^{-19}$seconds, particles usually neutrons, are "boiled" off. That is, it remains together until enough energy happens to be concentrated in one neutron to escape the mutual attraction. Charged particles rarely boil off because of the Coulomb Barrier. The excited quasi-bound nucleus is called a **Compound Nucleus**.A compound nucleus can decay in a number of different ways like Evaporation Residue, Fusion-Fission or Quasi-Fission. The compound nucleus has a long lifetime ($10^{-14}$ to $10^{-18}$sec) in reference to nuclear interaction time which is of much shorter duration.

It is relevant to mention here that, in general a compound nucleus does not depend on the composition of projectile and target nucleus and hence it is generally treated independent of entrance channel profiles. However in certain cases, depending on the shape and size of target-projectiles involved in nuclear reaction, some entrance channel effects has also been explored.

As the compound nucleus is always in an excited state, so complete understanding about this complex nuclear phenomena is quite difficult. Depending on various complexities involved at CN (compound nuclear) state, various decay mechanisms (modes) are possible.

## 1.3 Heavy-Ion Reactions:

The nuclear reaction in which the incident particle or target nucleus is a heavy-ion i.e. having atomic number, $Z \geq 2$ or atomic mass, $A \geq 4$ is known as a Heavy-Ion Reaction.Heavy ion reaction simply occurs when a projectile beam is incident on a target creating a compound nucleus which is relatively stable and highly excited with very high angular momentum.This compound nucleus then needs to lose some of this excess energy. Heavy-ion collisions have always played a fascinating role in exploring various aspects of fragment emission such as evaporation residue, fusion-fission, particle production, quasi-fission, multi-fragmentation, collective flow, etc [5].However as we confine ourselves to low energy dynamics only, so our analysis will be confined to ER (Evaporation Residue), Fusion-Fission and Quasi-Fission processes only.

## 1.5 Different possible Decay Modes of a Nucleus:

When a collision occurs between the incident particle/nucleus and a target nucleus, either the beam particle scatters elastically leaving the target nucleus in its ground state or the target nucleus is internally excited and subsequently decays by emitting radiations or nucleons. The different Decay Modes through which a nucleus can be decayed are:

- Evaporation Residue Mode
- Fusion-Fission Mode
- Quasi-Fission Mode

Beside this, one may have Particle Production, Deep Inelastic Collision (DIC) and Incomplete Fusion (ICF) etc. But in the present work, we focus on the first three only.

### 1.5.1 Evaporation Residue Mode:

Evaporation Residue is the main decay mode for a variety of nuclear systems formed via heavy ion reaction across the periodic table. Such decay prospects are more prevalent in mass range A≈40-100, where fission is generally absent. It is one of the important decay channel from compound nuclear state which comprises of particles in the range of A≤4 and Z≤2. In this process, the light particles like neutrons, Protons, deuterium, tritium and α-particle etc. having A≤4 and Z≤2 are emitted.

The process of Evaporation Residue occurs when a projectile beam is incident on a target, creating a compound nucleus which is relatively stable but excited with fairly large angular momentum and excitation energy.This compound nucleus now loses some of this excess energy in the form of alpha particles, neutron, proton and gamma rays. Normally if, available energy is sufficiently large, then alpha particle is emitted otherwise smaller particles like neutrons, protons etc. are emitted. As the system is in excited state so the stable condition is achieved via emission of gamma rays. The Evaporation Residue process is depicted below in figure 1.1.

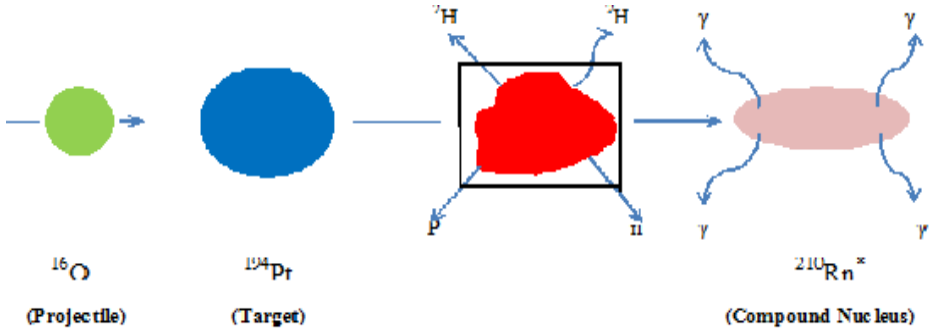


Fig 1.1 The Evaporation Residue decay mode

### 1.5.2 Fusion-Fission Mode:

For the heavy nuclear systems with A≈200 the most probable decay mode of the compound nucleus is fission, due to its instability against centrifugal repulsion. However for compound nuclear systems in range of A≈100-200, there is competition between ER (Evaporation Residue), Fission and IMF (Intermediate Mass Fragmentation) processes. Here IMF refers to intermediate mass fragments with Z=2-5, A=5-20. The energy of the two nuclei is conserved and remains

small during the motion through the Coulomb barrier. The penetration through this barrier is the main obstacle for low-energy Fusion [6]. These so-called fusion-evaporation and fusion-fission reactions represent the complete fusion-reaction channel of the colliding nuclei. The main difference between Evaporation Residue (shown in fig 1.1) and Fusion-Fission process is that we get highly asymmetric fragments in case of evaporation residue whereas fusion-fission results in decay fragments having comparable masses.

### 1.5.3 Quasi-Fission mode:

One type of reaction is the Deep-inelastic reaction. Deep-inelastic collisions of nuclei are very energetic collisions. Such reactions involve heavier ions and generally take place at intermediate impact parameter. For large impact parameter, they go over into the direct or Quasi-Elastic reaction and for small impact parameter into Fusion. The important difference between ER, Fission and Deep-inelastic reactions is that the compound nucleus(CN) formation take place in first two whereas third one is non-compound nucleus reaction. With this non-compound nucleus reaction (nCN) if the emitted products are identical with the formation partners, the reaction is called as Quasi-fission reaction or Quasi-fission process or we can define it as the system formed by the projectile and target nuclei can re-separate before complete fusion due to the strong repulsive Coulomb force in the so-called quasi-fission process. In general, the fragments from quasi-fission have significantly different mass and angular distributions than the fragments from a fusion-fission reaction [7].The Quasi-Fission Decay Mode is applicable at higher incident energies only.

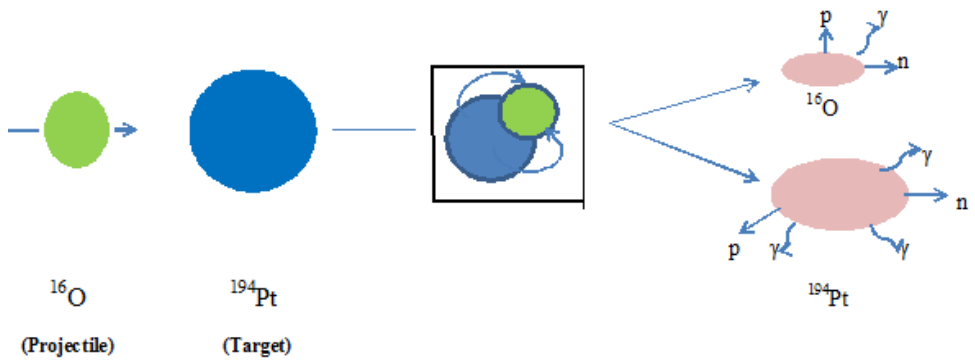


Fig 1.2 The Quasi-Fission Decay mode

In the quasi-fission process, incoming nuclei in a reaction do not loose its identity during the CN (Compound Nucleus) state and as a result such a non-equilibrated CN decays into fragments which are nearly the same as in the entrance channel i.e. projectile and target like fragments are emitted in the decay process. Several experimental studies show that the collision with tip to tip of deformed projectile-target nuclei lead to quasi-fission and the side collisions results in fusion-fission [8,9].The quasi-fission process is found to have a very strong entrance-channel dependence and is a major hurdle in the formation of super-heavy elements. The onset of these processes reduces the CN formation probability and hence the ER cross-section [10]. A systematic analysis of such kind of rare nuclear decay process is extremely important to have overall understanding of dynamics involved in the heavy ion reaction.

## 1.6 Comparative Analysis of Different Decay Modes

It is of immense interest to explore relative importance of competing decay modes in light, intermediate, heavy and Super-heavy mass region. Depending on the mass region of chosen nuclear reaction, Evaporation Residue (ER), Intermediate Mass Fragmentation (IMF), Heavy Mass Fragmentation (HMF), Fission, Quasi-Fission (QF) etc. could come into picture. Although Evaporation Residue is more prominent process at light mass region and fission is preferred for higher mass compound systems. For example, for $A<80$, Evaporation Residue is main contributor towards total decay cross-section and for $A\approx200$, fission supersedes all other decay mechanisms. But the relative contribution of different decay modes discussed in previous sections has always been of immense interest in the analysis of nuclear reaction dynamics and associated problems. Therefore, we have chosen a reaction $^{16}O+^{194}Pt\rightarrow^{210}Rn^{*}$ which exhibits the possibility of more than one decay path and hence comparative analysis of such a process is of interest.

## 1.7 Nuclear Deformations

Many nuclei are only slightly non-spherical, and so can still be well described by spherical nuclear models. However, for nuclei with a mass number A in the range 150<A<190 and A>220, the deformation effects can no longer be ignored. To lowest order, most deformed nuclei can be approximated as quadrupole deformed (i.e. a prolate or oblate ellipsoid).

Intrinsic quadrupole moment of evenly charged ellipsoid can be described by equation

$Q_0 = 2/5\ Z\ (b^2 - a^2)$,

where b is large, and a is small ellipsoid axes.

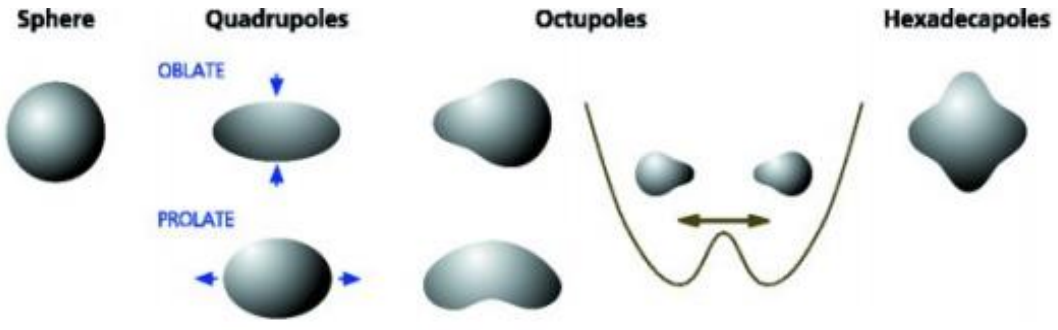


Fig 1.3Schematic diagram for various deformations in nuclei. For quadru-pole deformations, there are two choices i.e. nuclear matter rotates on short axis (oblate) and on long axis (prolate).

It is found that different shapes may coexist at the same spin and similar energies, which is considered to be the result of an interplay between a single particle and collective degrees of freedom [11],[12],[13],[14]. Hence, a mere spherical picture cannot reflect the real nuclear structure and related dynamics.

Nuclei having spherical shape in their ground state (g.s) are few in number [12]. The deformed nuclei are classified as prolate, oblate, and triaxial. Prolate and oblate nuclei are axially symmetric. For triaxial nuclei, the 3 axes are different. In nature, prolate nuclei dominate over oblate ones [13]. It is found that 86% of the even-even nuclei are prolate in the ground state [15]

and triaxial shapes are very rare for them. The effect of Coulomb repulsion between protons is to deform the nucleus into an elongated shape more than that to a flattened shape.

Deformation alters the properties of single-particle wave functions from those of the spherical shell model. In particular, the breaking of spherical symmetry changes the degeneracies of energy levels, and allows for collective rotation of the nucleus. The nuclear deformation plays an important role in the "geometry" of the collision [16].Deformed nuclei exhibit rotational bands as their lowest excitations, with actinides and rare earth nuclei being the most prominent [17].Figure 1.3 shows the schematic diagram for various deformations in nuclei.

The methodology used here in this dissertation i.e. Dynamical Cluster Decay Model (DCM) is discussed in detail in chapter 2. The deformation and orientation effects are duly incorporated within DCM.

It is relevant to mention here that the DCM has been applied successfully to study the decay of light, heavy and super heavy compound nuclei [18-25] referred in chapter 2. In the present work, the decay of heavy mass CN $^{210}Rn^{*}$ formed in $^{16}O+^{194}Pt$ reaction has been studied using DCM over a range of center-of-mass energies $E_{c.m.}$. As the data was available for Evaporation Residue (ER) and Complete fusion [10], so the same has been tested in the framework of DCM. The Fission cross-sections were fitted by subtracting ER cross-sections from complete fusion cross-sections. Deformation effects upto $\beta_2$ (quadrupole) were included within optimum orientation approach. Interestingly, some Quasi-Fission contribution is predicted at some higher two energies in context of chosen reaction.

## 1.8 References:


1. S. Hofmann and G. Munzenberg, Rev. Mod. Phys. 72, 733 (2000); Yu. Ts. Oganessian, J. Phys. G 34, R165 (2007); N Wang, E.G. Zhao, W. Scheid, and S.G. Zhou, Phys. Rev. C 85, 041601 (2012); K. P. Santhosh, B. Priyanka, J. G. Joseph and S. Sahadevan, ibid. 84, 024609 (2011).
2. H. Esbensen, Phys. Rev. C 85, 064611 (2012).
3. Y. Oguri, J. Hasegawa, K. Horioka, and S. Kawata [Nucl. Instr. Meth. Phys. Res. Sect. A 606, 1 (2009)].
4. Cheuk-Yin Wong, Phys. Rev. C 86, 064603 (2012).
5. Yogesh K. Vermani, Supriya Goyal, and Rajeev K. Puri- Phys. Rev. C 79, 064613 (2009).
6. B. Ivle, Phys. Rev. C 87, 034619 (2013).
7. J. Khuyagbaatar, K. Nishio, S. Hofmann, D. Ackermann, M. Block, S. Heinz, F.P. Heßberger, K. Hirose, H. Ikezoe, B. Kinlder, B. Lommel, H. Makii, S. Mitsuoka, I. Nishinaka, T. Ohtsuki, Phys. Rev. C 86, 064602 (2012).
8. D.J. Hinde, M. Dasgupta, J.R. Leigh, J.P. Lestone, J.C. Mein, C.R. Morton, J.O. Newton, and H. Timmers, Phys. Rev. Lett. 74, 1295 (1995).
9. V. I. Zagrebaev, A. V. Karpov, and Walter Greiner, Phys. Rev. C 81, 044608 (2010).
10. E. Prasad, K. M. Varier, N. Madhavan, S. Nath, J. Gehlot, Sunil Kalkal, Jhilam Sadhukhan, G. Mohanto, P. Sugathan, A. Jhingan, B. R. S. Babu, Varughese, K. S. Golda, B. P. Ajith Kumar, B. Satheesh, Santanu Pal, Singh, A. K. Sinha and S. Kailas, Phys. Rev. C84, 064606 (2011).
11. P.M. Walker, F.R. Xu and D.M. Cullen, Phys. Rev., C71, (2005), 067303.
12. R. Lucas, Europhysics News, 32, (2001), 5.
13. I. Maqbool, P. A. Ganai and J. A. Sheikh, DAE-BRNS Proceedings of Int. Symp. on Nucl. Phys., 54, (2009), 164.
14. H. Sagawa, X. R. Zhou and X. Z. Zhang, Phys. Rev., C72, (2005), 054311.
15. N. Tajima and N. Suzuki, Phys. Rev., C64, (2001), 037301.

16. Maciej Rybczynski, Wojciech Broniowski and Grzegorz Stefanek, Phys. Rev. C 87, 044908 (2013).
17. Jialin Zhang and T. Papenbrock, Phys. Rev. C 87, 034323 (2013).
18. R.K. Gupta, M. Balasubramaniam, R. Kumar, D Singh, C. Beck and W Greiner, Phys. Rev. C 71, 014601 (2005); and earlier references therein.
19. R.K. Gupta, M. Balasubramaniam, R. Kumar, D Singh, S K Arun and W Greiner, J. Phys. G, Nucl. Part. Phys. 32, 345 (2006).
20. B. B. Singh, M. K. Sharma, R. K. Gupta and W. Greiner, Int. J. Mod. Phys. E 15, 69(2006).
21. B. B. Singh, M. K. Sharma and R. K. Gupta, Phys. Rev. C 77, 054613 (2008).
22. R.K. Gupta, S. K. Arun, R. Kumar and Niyti, Int. Rev. Phys. (IREPHY) 2, 369 (2008).
23. R. Kumar and R.K. Gupta, Phys. Rev. C 79, 034602 (2009).
24. S. K. Arun, R. Kumar and R.K. Gupta, J. Phys. G: Nucl. Part. Phys. 36, 085105 (2009).
25. S. Kanwar, M. K. Sharma, B. B. Singh, R. K. Gupta and W. Greiner, Int. J. Mod. Phys. E 18, 1453 (2009).

# Chapter 2

# Methodology

# Chapter 2

# The Dynamical Cluster Decay Model (DCM)

## 2.1 Introduction

The Dynamical Cluster-Decay Model [1-8] (DCM) is an adaptation of the preformed cluster model (PCM) of Gupta et al. [9, 10] for ground- state decays, which itself is based on the well-known Quantum Mechanical Fragmentation Theory, the QMFT [11-13], given for fission and heavy ion reactions.

This theory of DCM is worked out in terms of the collective coordinates of mass and charge-asymmetries: $\eta = (A_1 - A_2) / (A_1 + A_2)$ and $\eta_Z = (Z_1 - Z_2) / (Z_1 + Z_2)$

Here in DCM, we define the decay cross-sec

tions in terms of the partial wave analysis as:

$$\sigma = \frac{\pi}{k^2} \sum_{\ell=0}^{\ell_{max}} (2\ell + 1) P_0 P \qquad (1)$$

with $k$ given by .

The reduced mass, $$k = \sqrt{\frac{2\mu E_{c.m}}{\hbar^2}}$$

$$\mu = [A_1 A_2 / (A_1 + A_2)]m = \frac{1}{4} Am(1 - \eta^2)$$

where m is the nucleon mass and $\ell_{max}$ as the maximum angular momentum which could be used as a free parameter or else fixed for the vanishing of the fusion barrier of the incoming channel $\eta_i$ or the light particle cross section $\sigma_{LP} \rightarrow 0$.

For $\eta$-motion, we solve the stationary Schrödinger equation in $\eta$, at a fixed R,

$$\left\{ -\frac{\hbar^2}{2\sqrt{B_{\eta\eta}}} \frac{\partial}{\partial \eta} \frac{1}{\sqrt{B_{\eta\eta}}} \frac{\partial}{\partial \eta} + V_R(\eta, T) \right\} \psi^{\nu}(\eta) = E^{\nu} \psi^{\nu}(\eta) \qquad (2)$$

with $\nu = 0,1,2,3,\ldots..$ referring to ground state( $\nu = 0$) and excited state solutions.

The deformation and orientation dependent fragmentation potential at any temperature is given as:

$$V_R(\eta,T) = \sum_{i=1}^{2}[V_{LDM}(A_i,Z_i,T)] + \sum_{i=1}^{2}[\delta U_i]\exp(-T^2/T_0^2) + V_c(R,Z_i,\beta_{\lambda i},\theta_i,T) + V_P(R,A_i,\beta_{\lambda i},\theta_i,T) + V_\ell(R,A_i,\beta_{\lambda i},\theta_i,T) \quad (3)$$

where the $T$-dependent liquid drop energy $V_{LDM}(T)$ is that of Ref. [14], with (Seeger's) constants at $T = 0$ refitted to give binding energies of [15], defined as $B = V_{LDM}(T=0) + \delta U$. The shell corrections are calculated in the "empirical method'' of Myers and Swiatecki [16].

The $V_P$ is an additional attraction due to the nuclear proximity potential [17], which is also considered temperature dependent here,

$$V_P(s_o(T)) = 4\pi\bar{R}(T)\gamma b(T)\phi(s_o,(T)), \quad (4)$$

where $\bar{R}(T)$ and $\phi(s_o,T)$ are, respectively, the inverse of the root mean square radius of the Gaussian curvature and the universal function, which is independent of the geometry of the system.

The same temperature dependence of $R(T)$ is also used for Coulomb potential $E_c(T) = Z_1Z_2e^2/R(T)$, where the charges $Z_i$ are fixed by minimizing the potential $V_R(\eta,T)$ in the charge asymmetry coordinate $\eta_Z = (Z_1 - Z_2)/(Z_1 + Z_2)$. The shell corrections $\delta U$ in the Eq. (3) are considered to vanish exponentially for $T_0 = 1.5$ Mev.

Also, for the angular momentum effects

$$V_\ell(\mathrm{T}) = \frac{\hbar^2\ell(\ell+1)}{2I(T)} \quad (5)$$

In the non-sticking limit, where $R_a = R_1(T) + R_2(T) + \Delta R = R_t(T) + \Delta R$, the moment of

inertia in Eq.(5) is given by

$$I\ (T) = I_{NS}(T) = \mu \mathrm{R_a}^2 \quad (6)$$

In this case, the separation distance ΔR is assumed to be beyond the range of nuclear proximity forces, which is about 2 fm. However, when it is within the range of nuclear proximity (< 2 fm), we get moment of inertia in the complete sticking limit as

$$I\ (T) = I_S(T) = \mu \mathrm{R_a}^2 + \frac{2}{5}\mathrm{A_1 m R_1}^2 + \frac{2}{5}\mathrm{A_2 m R_2}^2 (7)$$

The eigen-solutions of Eq. (2) give the preformation probability

$$P_0 = \sqrt{B_{\eta\eta}}\left|\psi[\eta(A_i)]\right|^2 (2/A) \quad (8)$$

($i$ =1 or 2), where $\psi(\eta)$ is $\psi^{\nu=0}(\eta)$ if the ground-state solution is chosen.

The mass parameters $B_{\eta\eta}(\eta)$, representing the kinetic energy part in Eq.(2), are the smooth classical hydro-dynamical masses [18], since at high temperatures the shell effects are almost washed out.

At temperature $T$, the preformation factor $P_0$ in Eq. (8) is calculated at $R_a = R_t(\eta)+\Delta R$, with the temperature effects also included in $\psi(\eta)$ through a Boltzmann-like function

$$\left|\psi\right|^2 = \sum_{\nu=0}^{\infty}\left|\psi^{\nu}\right|^2 \exp(-E^{\nu}/T), (9)$$

For the decay of a hot compound nucleus, the first turning point R = $R_a$where $P_0$ calculated is defined as,

$$R_a = R_1(\alpha_1,T) + R_2(\alpha_1,T) + \Delta R(\eta,T),$$

$$= R_t(\alpha, \eta, T)+\Delta R(\eta,T), \quad (10)$$

with radius vectors

$$R_i(\alpha_i, T) = R_{0i}(T)\left[1+\sum_{\lambda}\beta_{\lambda i}Y_{\lambda}^{(0)}(\alpha_i)\right]$$

The temperature dependence in radii $R_i$ are given as [19]

$$R_{0\,i} = [1.28A_i^{1/3} - 0.76 + 0.8A_i^{-1/3}](1+0.0007T^2) \quad (11)$$

with the surface width

$$b(T) = 0.99(1+0.009T^2) \quad (12)$$

This value of $R$ (instead of the compound nucleus radius $R_0$) assimilates to a good extent the effects of both deformations $\beta_i$ of two fragments and neck formation between them [19].In the definition of *Ra* above, $\Delta R$ is the relative separation distance between two fragments or clusters $A_i$. In the language of the two-center shell model, used to determine shell effects $\delta U$, $\Delta R$ is shown to assimilate the neck formation effects [20, 21], and hence is referred to as the neck-length parameter. This is more true for fission fragments and not for a neutron cluster as one of the fragments, but is similar to that used in both the scission-point [22] and saddle-point [23,24] statistical fission models for calculating the ER and fission cross sections. It is worth noting that the ΔR are higher for the simultaneous fitting of the Evaporation Residue and Fission processes than for independent fitting of each process. (discussed in chapter 3). The potential corresponding to $R_a, V(R_a)$ acts like an effective, positive $Q$ value, $Q_{eff}$, for the decay of the hot compound nucleus at temperature $T$ to two fragments in the exit channel observed in the ground states $(T=0)$. Thus, in terms of the respective binding energies $B$, $Q_{eff}$ is defined as

$$\Delta\, Q_{eff}(T) = B(T) - [B_1(T=0) + B_2(T=0)]$$

$$= TKE(T) = V(R_a) \quad (13)$$

Since,$R_a = R_t(\eta)$ for $T = 0$, and $\Delta R(\eta)$ corresponds to the change in $TKE$ at $T$ with respect to its value at $T = 0$, and hence can be estimated exactly for the temperature effects in the scattering potential $V(R)$.

For the penetrability $P$,

$$V(R_a) = V(R_t + \Delta R) = V(R_b) = Q_{eff} = TKE(T) \qquad (14)$$

With $R_b$ as the second turning point. The penetrability $P$ is calculated as the WKB tunneling probability, solved analytically in Ref. [9, 10], as

$$P = \exp[-\frac{2}{\hbar}\int_{R_a}^{R_b}\{2\mu[V(R)-Q_{eff}]\}^{1/2}dR] \qquad (15)$$

And finally,

The compound nucleus temperature $T$ (in MeV) related as

$$E_{CN}^{*} = \left(\frac{A}{9}\right)T^2 - T \qquad (16)$$

## 2.2 References:

1. R.K. Gupta, M. Balasubramaniam, R. Kumar, D Singh, C. Beck and W Greiner, Phys. Rev. C 71, 014601 (2005); and earlier references therein.

2. R.K. Gupta, M. Balasubramaniam, R. Kumar, D Singh, S. K. Arun and W. Greiner, J. Phys. G: Nucl. Part. Phys. 32, 345 (2006).

3. B. B. Singh, M. K. Sharma, R. K. Gupta and W. Greiner, Int. J. Mod. Phys. E 15, 699 (2006).

4. B. B. Singh, M. K. Sharma and R. K. Gupta, Phys. Rev. C 77, 054613 (2008).

5. R.K. Gupta, S. K. Arun, R. Kumar and Niyti, Int. Rev. Phys. (IREPHY) 2, 369 (2008).

6. R. Kumar and R.K. Gupta, Phys. Rev. C 79, 034602 (2009).

7. S. K. Arun, R. Kumar and R.K. Gupta, J. Phys. G: Nucl. Part. Phys. 36, 085105 (2009).

8. S. Kanwar, M. K. Sharma, B. B. Singh, R. K. Gupta and W. Greiner, Int. J. Mod. Phys. E 18, 1453 (2009).

9. R.K. Gupta,Proc. $5^{th}$Int. conf. on Nuclear Reaction Mechanisms, Varenna, P 416 (1988).

10. S. S. Malik and R. K. Gupta, Phys. Rev. C 39,1992 (1989).

11. J. Maruhn and W. Greiner, Phys. Rev. Lett. 32, 548 (1974).

12. R.K Gupta, W. Scheid, and W. Greiner, Phys. Rev. Lett. 35, 353 (1975).

13. R.K. Gupta and W. Greiner, Heavy Elements and Related New Phenomena, WorldScientific, Singapore, edited by W. Greiner and R.K Gupta, Vol. I, P 397; P 536 (1999).

14. N.J. Davidson, S.S. Hsiao, J. Markram, H.G. Miller, and Y. Tsang, Nucl. Phys. A570, 61C (1994).

15. G. Audi and A.H. Wapstra, Nucl. Phys. A595, 4 (1995).

16. W. Myers and W.J. Swiatecki, Nucl. Phys. A81, 1 (1966).

17. J. Blocki, J. Randrup, W.J. Swiatecki, and C. F. Tsang, Ann. Phys. (NY) 105, 427 (1977).

18. H. Kroger and W. Scheid, J. Phys. G: Nucl. Phys. 6, L85 (1980).

19. G. Royer and J. Migner, J. Phy. G 18, 1781 (1992), and earlier references therein.

20. S. Kumar and R.K. Gupta, Phys. Rev. C 55, 218 (1997).

21. R. K. Gupta, S. Kumar, and W. Scheid, Int. J. Mod. Phys. E 6, 259 (1997).

22. T. Matsuse, C. Beck, R. Nouicer, and D. Mahboub, Phys. Rev. C 55, 1380 (1997).

23. S. J. Sanders, Phys. Rev. C 44, 2676 (1991).

24. S. J.Sanders, D. G. Kovar, B. B. Back, C. Beck, D. J. Henderson, R. V. F. Janssens, T. F. Wang, and B. D. Wilkins, Phys. Rev. C 40, 2091 (1989).

# Chapter 3

# Results & Conclusions

# Chapter-3

# Results and Discussions

## 3.1 Introduction:

In this chapter, we have investigated the dynamics of $^{16}O+^{194}Pt$ reaction using Dynamical Cluster Decay Model (DCM) over a wide range of incident energies above the Coulomb barrier.

Recently, the Evaporation Residue cross-sections for the decay of $^{210}Rn^{*}$ have been measured over a wide range of energies in [1]. Along with the experimental Evaporation Residue cross-sections, the complete fusion cross-sections calculated by using CCFULL is available. Here in the present work, the decay of $^{210}Rn^{*}$ is studied in reference to [1]. The Evaporation Residue as well as Fission cross-sections are calculated using collective clusterization approach using DCM. The fission cross-sections are estimated by subtracting the Evaporation Residue cross-sections from CCFULL calculated Complete Fusion Cross-sections and the same have been tested using DCM. The calculations are done by considering the quadrupole deformation ($\beta_2$) within optimum orientation approach. The following points are investigated:

1. Evaporation Residue and Fission cross-sections are calculated by independently fitting the neck length parameter, $\Delta R$ at different energies for compound nucleus $^{210}Rn^{*}$ formed in the reaction $^{16}O+^{194}Pt$ in reference to data of [1].
2. Following this, the Cross-sections are calculated by simultaneously fitting the neck length parameter for the Evaporation Residue and Fission decay modes at lowest energy. The simultaneous choice of $\Delta R$ doesn't seem to work at higher incident energies.
3. The effect of Quasi-Fission is observed at higher energies.

The available Cross-sections are fitted in reference to the experimental data by fitting Neck-Length Parameter, $\Delta R$ using DCM [2-10]. It is the only parameter of model which generally increaseswith the increase of $E_{c.m.}$. Comparative study is done for compound nucleus $^{210}Rn^{*}$ in terms of fragmentation potential ($V_\eta$), preformation probability ($P_0$) and cross-sections ($\sigma$) and Angular Momentum ($\ell$) dependence of the $^{16}O+^{194}Pt$ reaction by taking independent and simultaneous choice of neck length parameter $\Delta R$ for fitting Evaporation Residue (ER) and Fission data.

## 3.2 Evaporation Residue and Fission Decay:

### 3.2.1Evaporation Residue calculations:

We started with fitting the Evaporation Residue cross-sections. In other words, the neck length parameter ΔR was chosen such that calculated Evaporation Residue cross-sections start comparing with experimental data of [1].

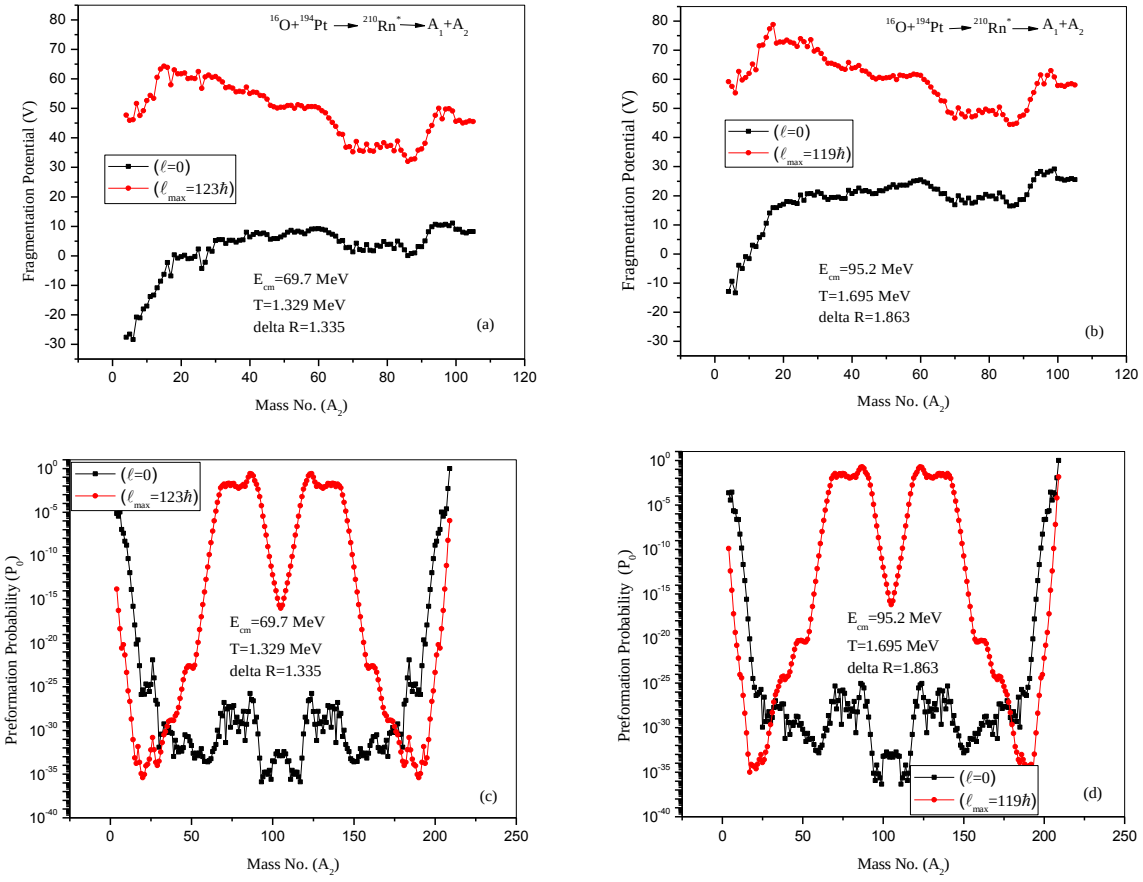


Fig.3.1 The comparison of Fragmentation Potential and Preformation Probability for lowest and highest energies for Evaporation Residue Cross-Section only.

First of all, we look for fragmentation path for the decay of $^{210}Rn^{*}$ formed in $^{16}O+^{194}Pt$ reaction. Fig 3.1(a & b) shows the comparison between the fragmentation potential as a function of atomic mass at lowest energy, $E_{c.m.}$=69.7 MeV and highest energy, $E_{c.m.}$=95.2 MeV.

It is clear from Fig 3.1 that the structure of potential energy surface remains similar independent of the energy at $\ell$=0 and at $\ell=\ell_{max}$ value, though the magnitude is larger for the higher incident energy. It can further be seen from the figure that at $\ell$=0, light particles are more probable whereas fission starts competing at higher $\ell$-values. Also asymmetric distribution is preferred in the decay of $^{210}$Rn independent of energy.This is further clear from Fig 3.1 (c & d) showing the preformation probability as a function of light mass fragment at lowest and highest energy that the asymmetric fragments in the range ($A_2$= 68-91 and complementary fragments) are contributing towards fission cross-sections independent of the energy of incident projectile. The contribution of symmetric fragments towards fission is observed to be negligibly small. It is worth noting that deformation effects upto $\beta_2$ (quadrupole) are included in these calculations, so the effect of shape and configuration of decaying fragments is duly incorporated in this work.

### 3.2.2 Fission Cross-Section calculations:

Recently [1], the Evaporation Residue cross-sections were measured and complete fusion cross-sections were estimated within CCFULL code. The fission cross-sections are estimated by subtracting the experimental Evaporation Residue cross-sections from the CCFULL calculated complete fusion cross-sections. This can be seen as:

$$\sigma_{fusion} = \sigma_{CF}(\text{CCFULL}) - \sigma_{ER}(\text{expt})$$

In this section, we have addressed the fission data using DCM approach.

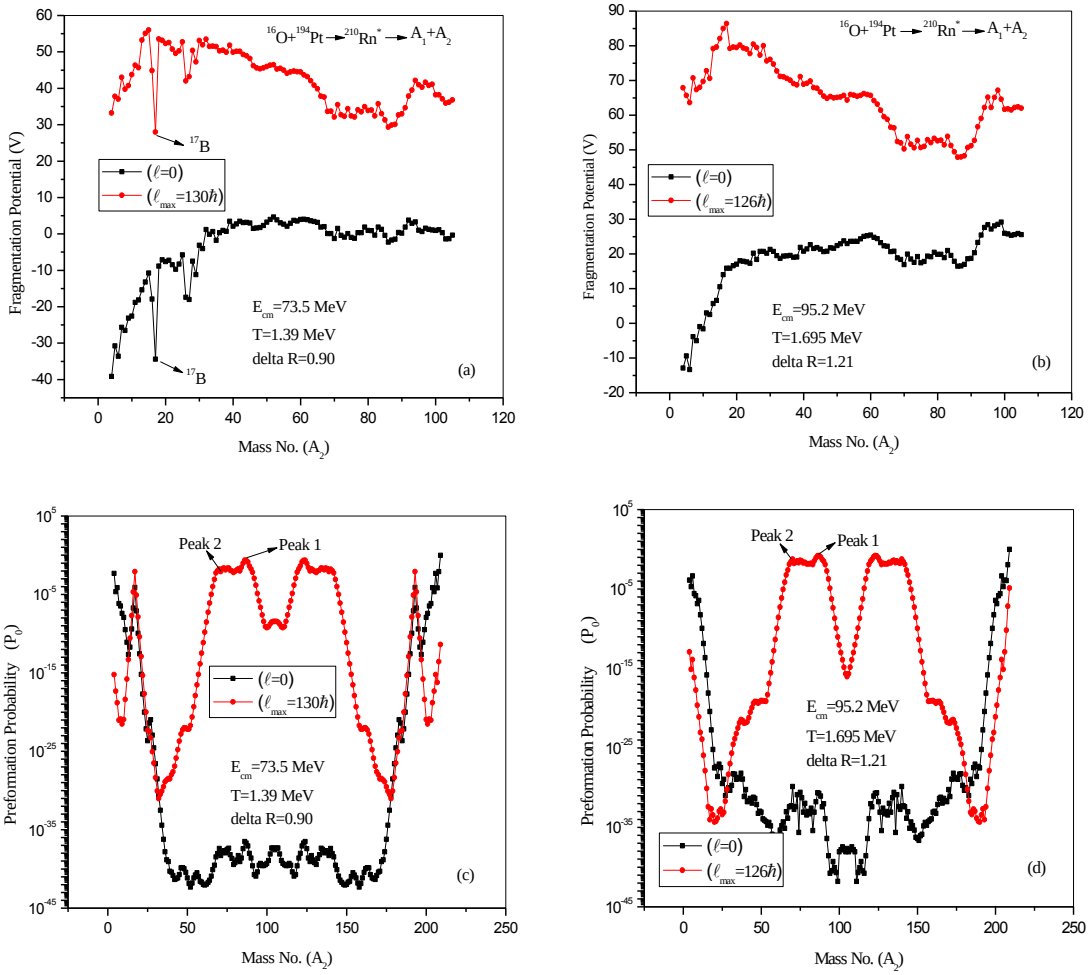


Fig. 3.2 The comparison of Fragmentation Potential (V) and Preformation Probability ($P_0$) at lowest and highest energies for fitting of Fission cross-sections data.

Figure 3.2 (c & d) shows the preformation probability as a function of light mass fragment at lowest and highest energy for the case of fission process which shows that the asymmetric fragment in the range ($A_2$= 68 to 91) are contributing towards fission cross-sections independent of the energy. This trend is similar to Fig 3.1(c & d) obtained for Evaporation Residue case. However there is an interesting observation in Fig 3.2 (c), here at lowest energy, the fitting of fission cross-section suggest that relative contribution of symmetric and near-symmetric fission fragments have enhanced in comparison to that for Evaporation Residue (ER) fitting. Beside this, another peak is observed in IMF (Intermediate Mass Fragment) region near the mass of projectile, A=16. Also, from the fig 3.2 (a & b), the curve for fragmentation potential as a function of mass fragment shows that potential energy surface is nearly same at both ℓ=0 and

$\ell=\ell_{max.}$It is clear from the fragmentation curve that the decay pattern of $^{210}Rn^{*}$ is similar at both the energies with some difference in magnitude only. However, the dip obtained at $A_2$=17 i.e. $^{17}B$ is missing in the Evaporation Residue case. The presence of this dip might be due to the inappropriate choice of deformation for this fragment. The peak around A=16 in preformation plot is possibly due to emergence of this and nearby fragments.

The Evaporation Residue and Fission cross-sections calculated within DCM find nice agreement with the available data at all energies except for Fission cross-sections at the two highest energies wherecalculated cross-sections are underestimated in reference to available data [1]. This disagreement between DCM and available data seems to suggest that some other competing decay channel might be in operation at highest two energies. One of the possibility is Quasi-Fission.

The DCM calculated cross-sections are compared with the available data for Fission and Evaporation Residue in figure 3.3.

Fig 3.3 shows the comparison of DCM calculated cross-sections with experimental data.

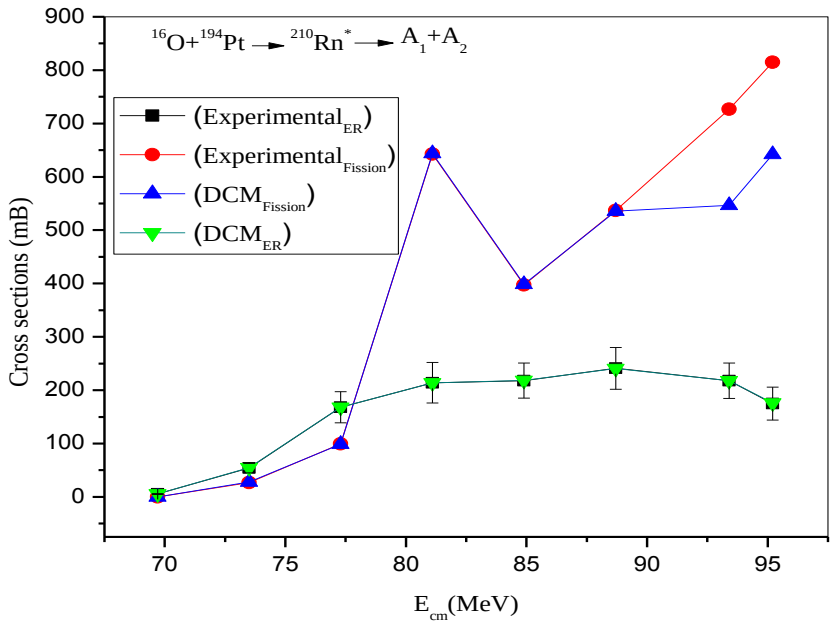


Fig. 3.3 DCM based cross-sections and experimental data for the $^{16}O+^{194}Pt\rightarrow^{210}Rn^{*}$.

From the Figure 3.3 and Tables 3.1 & 3.2, it is clear that the DCM calculated and experimental cross-sections for Evaporation Residue find nice comparison at all the energies. The calculated Fission cross-sections also find nice agreement with data [1], except for highest two energies. We have addressed this discrepancy in terms of Quasi-Fission contribution later in section 3.5.

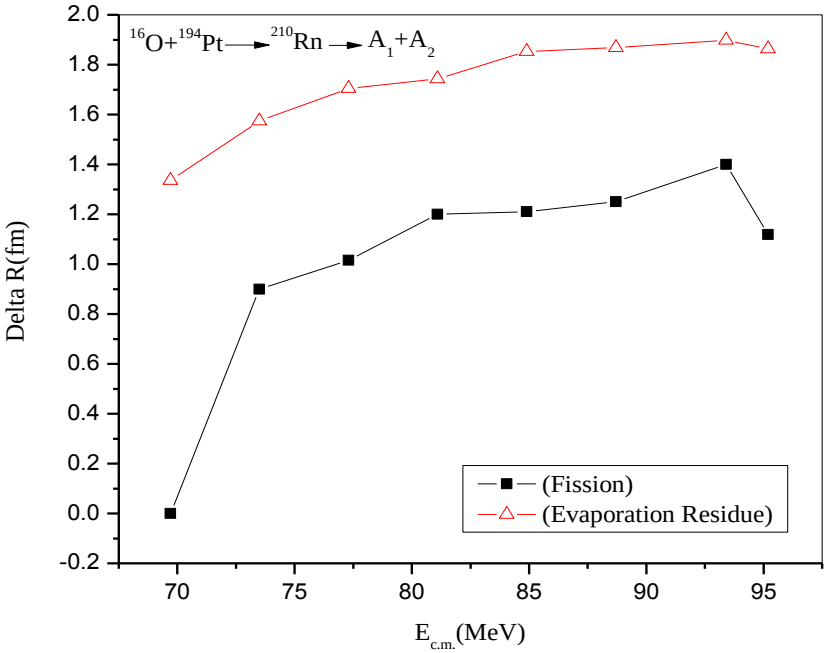


Fig. 3.4 The variation of Neck- Length Parameter (ΔR) with Energy ($E_{c.m.}$) for fitting of Evaporation Residue and Fission cross-sections.

In framework of DCM, the cross-sections are calculated by fitting the Neck-Length Parameter, ΔR. It is the only parameter of the model which takes care of the penetration point through the barrier. Fig. 3.4 shows the variation of ΔR as a function of energy. It can be seen from Fig. 3.4 that the ΔR value is larger for Evaporation Residue process as compared to that for Fission decay. This larger value of Evaporation Residue (ER) simply means that the ER process occurs first i.e. the ΔR value gives the time scale of the decay process. Beside this, the ΔR seems to vary as smoothing function of center of mass energy for Evaporation Residue as well as for Fission. A steep fall at highest energy in case of Fission seems to suggest that some competing channel is in operation at nearby energies as discussed in the previous section.

Table 3.1 Table showing the comparison between experimental Evaporation Residue cross-sections and calculated Evaporation Residue cross-sections using DCM.

| $E_{cm}$(MeV) | T(MeV) | $\Delta R_{ER}$(fm) | $\ell_{max}$ | $\sigma_{ER}$(DCM) | $\sigma_{ER}$(EXP) |
|---|---|---|---|---|---|
| 69.7 | 1.329 | 1.335 | 123 | 5.39 | 5.5±0.9 |
| 73.5 | 1.390 | 1.574 | 123 | 54.86 | 54.0±9.0 |
| 77.3 | 1.448 | 1.704 | 122 | 168.19 | 168.1±29.0 |
| 81.1 | 1.504 | 1.743 | 121 | 213.57 | 214.0±38.1 |
| 84.9 | 1.558 | 1.853 | 119 | 218.43 | 218.0±33.0 |
| 88.7 | 1.610 | 1.869 | 118 | 240.79 | 241.0±39.0 |
| 93.4 | 1.672 | 1.898 | 117 | 217.84 | 218.0±33.2 |
| 95.2 | 1.695 | 1.863 | 119 | 175.89 | 175.0±31.0 |

Table 3.2 Table showing the comparison between DCM calculated Fission Cross-sections compared with the available data.

| $E_{cm}$(MeV) | T(MeV) | $\Delta R_{fission}$(fm) | $\ell_{max}$ | $\sigma_{fission}$(DCM) | σ(quasi fission) | $\sigma_{fission+}\sigma_{quasi-fission}$(DCM) | $\sigma_{fission}$ = $\sigma_{fusion(CCFULL)}$-$\sigma_{ER}$(Exp) |
|---|---|---|---|---|---|---|---|
| 69.7 | 1.329 | - | - | - | - | - | - |
| 73.5 | 1.390 | 0.90 | 130 | 27.90 | - | 27.76 | 26.57 |
| 77.3 | 1.448 | 1.016 | 128 | 98.56 | - | 98.56 | 99.57 |
| 81.1 | 1.504 | 1.20 | 127 | 644.0 | - | 644.0 | 642.80 |
| 84.9 | 1.558 | 1.21 | 126 | 398.6 | - | 398.6 | 397.14 |
| 88.7 | 1.610 | 1.25 | 125 | 535.58 | - | 535.58 | 536.98 |
| 93.4 | 1.672 | 1.4 | 115 | 546.5 | 180 | 726.5 | 726.88 |
| 95.2 | 1.695 | 1.119 | 126 | 642 | 172 | 814 | 814.92 |

## 3.3 Simultaneous Fitting of ER and Fission Cross-Sections:

In addition to independent fitting of Evaporation Residue and Fission, an attempt is made to calculate the cross-section by simultaneously fitting the Neck-Length Parameter for Evaporation Residue and Fission.

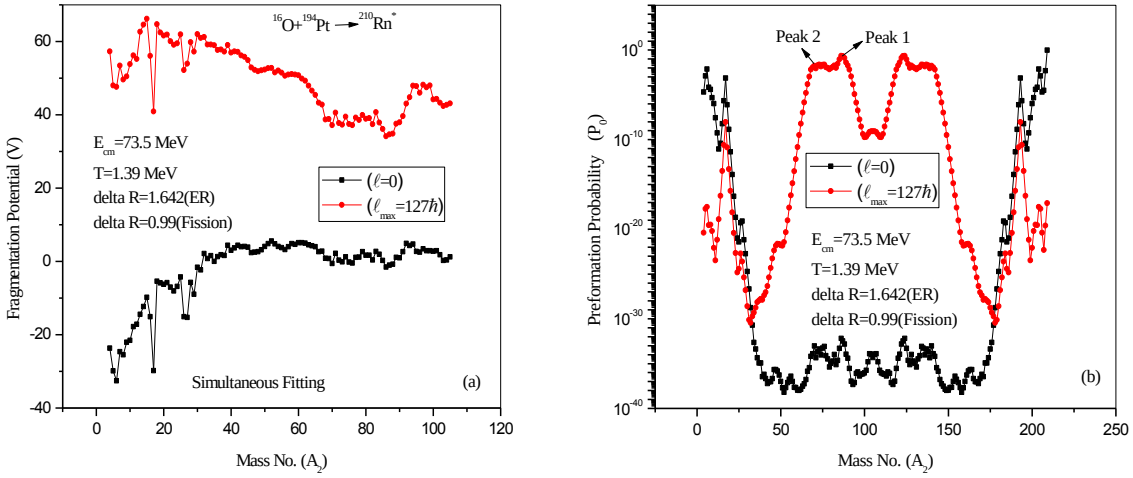


Fig. 3.5 The Variation of Fragmentation Potential (Vη) and Preformation Probability ($P_0$) and as a function of Mass No. ($A_2$) at lowest energy, $E_{c.m.}$=73.5 MeV when Evaporation Residue and Fission decay were worked out simultaneously.

Fig 3.5 shows the Fragmentation Potential and Preformation Probability as a function of fragment mass for the simultaneous fitting of ΔR. It can be seen from Fig 3.5 (a & b) that the Potential Energy Surface (PES) (fragmentation) and preformation is similar to one obtained for the fission case i.e. there is no variation in the structure when one does calculations by simultaneously fitting the ΔR or by independently fitting of ΔR for fission decay. The peak around A=16 (projectile mass) is again visible in these calculations. However in collective clusterization approach, the effective contribution of this peak is negligibly small. The small difference in magnitudes can be seen. We could fit the available data on Evaporation Residue and Fission simultaneously at lower incident energies but the same was not true for higher energies. Therefore, the simultaneous fitting of Evaporation Residue and Fission also suggest that some competing channel is coming in operation at higher incident energies. This issue is discussed further in next section. Another point of interest in all preformation curves Fig 3.1 (c, d), 3.2 (c, d), 3.5 (b) is the emergence of some fine-(sub) structure among fissioning nuclei. This

trend of sub structure of fission fragments is of huge importance as contribution of individual fragments is being made available in present day data. An experimental verification of such structuring in fission region could be of interest for overall understanding of dynamics involved in context of this reaction.

## 3.4 Peak Ratio in Fissioning Region:

The fission fragments in the $\beta_2$-deformed path results in an asymmetric peak and a near-symmetric peak which gives rise to possibilities of substructure among fission fragments. It is clearly seen from the figure 3.2 (c & d) that a double humped fission distribution for $\beta_2$-deformed path is present and the fragments $A_2$=68-91 seems to contribute toward fission cross-sections. The substructure is analysed among fission fragments by calculating the asymmetric and near symmetric peak ratio (peak $_2$/peak $_1$) at all the energies. Figure 3.6 shows the values of peak ratios as a function of center of mass energy $E_{cm}$.

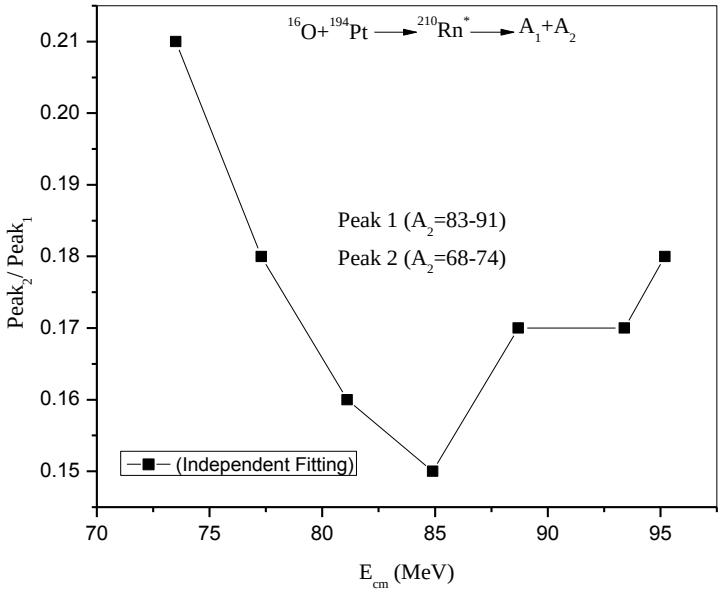


Fig 3.6 The ratio of the peak valuesof asymmetric fragments and near symmetric fragments as a function of $E_{cm}$.

It is clear from the figure 3.2 (c & d) & 3.5 (b) that Peak 1 ($A_2$=83-91) contributes more than Peak 2 ($A_{2=}$68-74) towards fission cross-sections. The contribution of near symmetric fission fragments dominates the fission cross-sections at all energies since the $peak_2/peak_1$ ratio is less than 1. However, it decreases with increase in energy till $E_{cm}$=84.9 MeV afterwards starts increasing. The contribution of in-between fragments $A_2$=75-82 is quite small. This is the observation for independent fitting of two (Evaporation Residue and Fission) decay processes, however for simultaneous fitting at one lowest energy, $E_{cm}$=73.5 MeV, give the $Peak_2$/ $Peak_1$ ratio equal to 0.28 which is larger than for independent fitting at the energy, $E_{cm}$=73.5 MeV. This shows relatively larger contribution of asymmetric fragments in simultaneous fitting.

## 3.5 Quasi-Fission:

Now, the disagreement between the DCM calculated cross-sections and available data at highest two energies have raised a call for some competing non compound nucleus contribution and the same is analysed here in the form of Quasi-Fission component. The Quasi-Fission cross-sections have been calculated at highest two energies by fitting the ΔR for the entrance channel fragments with $P_0$=1. It is so because in Quasi-Fission, outgoing fragments are identical to that of incoming channel. It has been observed that by adding the Quasi-Fission to the DCM calculated fission component, the DCM calculations are compared nicely with available data. The Quasi-Fission contribution at highest two energies is depicted in table 3.2. The Quasi-Fission component for the highest two energies in the reaction $^{16}O+^{194}Pt\rightarrow^{210}Rn^*$ is fitted by taking the neck-length parameter, ΔR=1.14 for $E_{cm}$=93.4 MeV and ΔR=1.12 for $E_{cm}$=95.2 MeV.

## 3.6Summary:

In Summary, the decay of $^{210}Rn^*$ nuclear system formed in $^{16}O+^{194}Pt$ reaction is studied over a wide range of incident energies using DCM. The Evaporation Residue and Fission cross-sections are calculated in reference to experimental data both by independently and simultaneously fitting of ΔR (neck length parameter), the only parameter of the model. The calculations, done by considering the quadrupole deformation ($\beta_2$), find nice agreement with the available data at all

the energies except for fission at two highest energies. On addition of the quasi fission component predicted at the highest two energies in the fission cross section, DCM based cross-sections find nice comparison with the available data. The fragmentation path and preformation shows that asymmetric distribution is preferred independent of the energy and fitting procedure. The $\Delta R$ is observed to increase with energy for both the processes being higher for Evaporation Residue process which implies Evaporation Residue occurs first at an early stage as compared to that for Fission decay. The contribution of near symmetric fragments is more than the asymmetric fragments. Some fine (sub)-structure is seen in the fission distribution independent of incident energy and fitting procedure. An experimental verification of such structuring effects in the fission region could be of future interest.

## 3.7References:

**1.** E. Prasad, K. M. Varier, N. Madhavan, S. Nath, J. Gehlot, Sunil Kalkal, Jhilam Sadhukhan, G. Mohanto, P. Sugathan, A. Jhingan, B. R. S. Babu, T. Varughese, K. S. Golda, B. P. Ajith Kumar, B. Satheesh, Santanu Pal, R. Singh, A. K. Sinha and S. Kailas, Phys. Rev.C **84**, 064606 (2011).

**2.** M. K. Sharma, G. Sawhney, R. K. Gupta, and W. Greiner, J.Phys. G: Nucl. Part . Phys. 38, 105101 (2011); M. K. Sharma, G. Sawhney, S. Kanwar, and R. K. Gupta, Mod. Phys. Lett. A 25, 2022(2010).

**3.** M. Kaur, R. Kumar, and M. K. Sharma, and M. K. Sharma, Phys. Rev. C 85, 014609(2012).

**4.** B. B. Singh, M. K. Sharma, R. K. Gupta and W. Greiner, Int. J. Mod. Phys. E 15, 699 (2006).

**5**. B. B. Singh, M. K. Sharma and R. K. Gupta, Phys. Rev. C 77, 054613 (2008).

**6.** K. Sandhu, M. K. Sharma, and R. K. Gupta, Phys. Rev. C 85, 024604 (2012).

**7.** R. Kumar and R.K. Gupta, Phys. Rev. C 79, 034602 (2009).

**8.** M. K. Sharma, G. Sawhney, S. Kanwar, R. K. Gupta, and W. Greiner, J. Phys. G: Nucl. Part. Phys. 38, 055104(2011); D. Jain, R. Kumar, M. K. Sharma, and R. K. Gupta, Phys. Rev. C 85, 024615(2012).

**9.** M. Kaur, Manoj K. Sharma, And Raj K. Gupta, Phys. Rev. C 86, 064610 (2012).

**10.** G. Kaur and M. K. Sharma, Nucl. Phys. A 884,36 (2012).